

Assembling Novel Heterotrimetallic Cu/Co/Ni and Cu/Co/Cd Cores Supported by Diethanolamine Ligand in One-Pot Reactions of Zerovalent Copper with Metal Salts

Dmytro S. Nesterov,[†] Valeriya G. Makhankova,[†] Olga Yu. Vassilyeva,^{*,†} Vladimir N. Kokozay,[†] Larisa A. Kovbasyuk,[‡] Brian W. Skelton,[§] and Julia Jezierska^{||}

Department of Inorganic Chemistry, National Taras Shevchenko University, Volodymyrska street 64, Kyiv 01033, Ukraine, Anorganisch-Chemisches Institut der Universität Heidelberg, Im Neuenheimer Feld 270, D-69120 Heidelberg, Germany, Chemistry, University of Western Australia, Crawley, Western Australia 6009, Australia, and Faculty of Chemistry, University of Wrocław, 14 Joliot-Curie Street, 50-383 Wrocław, Poland

Received August 2, 2004

The three novel heterotrimetallic complexes $[\text{Ni}(\text{H}_2\text{L})_2][\text{CoCu}(\text{L})_2(\text{H}_2\text{L})(\text{NCS})]_2(\text{NCS})_2$ (**1**), $[\text{Ni}(\text{H}_2\text{L})_2][\text{CuCo}(\text{L})_2(\text{H}_2\text{L})(\text{NCS})]_2\text{Br}_2 \cdot 2\text{H}_2\text{O}$ (**2**), and $[\text{CuCoCd}(\text{H}_2\text{L})_2(\text{L})_2(\text{NCS})\text{Br}_2] \cdot \text{CH}_3\text{OH}$ (**3**) have been prepared using zerovalent copper; cobalt thiocyanate; nickel thiocyanate (**1**), nickel bromide (**2**), or cadmium bromide (**3**); and methanol solutions of diethanolamine in air. The most prominent feature of the structures of **1** and **2** is the formation of the “pentanuclear” aggregate $\{[\text{Ni}(\text{H}_2\text{L})_2][\text{CoCu}(\text{L})_2(\text{H}_2\text{L})(\text{NCS})]_2\}^{2+}$ made up of two neutral $[\text{CoCu}(\text{L})_2(\text{H}_2\text{L})(\text{NCS})]$ units and the previously unknown cation $[\text{Ni}(\text{H}_2\text{L})_2]^{2+}$ “glued together” by strong complementary hydrogen bonds. With Cd^{2+} instead of Ni^{2+} , a different structure is obtained: the $[\text{CoCu}(\text{L})_2(\text{H}_2\text{L})(\text{NCS})]$ unit is now linked to the Cd center through coordination of the oxygens of L groups on the Co atom to form the discrete heterotrimetallic molecular species **3**. Cryomagnetic measurements of the compounds show that, in all cases, the magnetic behavior is paramagnetic; the polycrystalline EPR spectra contain signals due to monomeric copper species only. At the same time, the EPR spectra of frozen DMF and methanol solutions of **1–3** reveal the presence of triplet-state species that can be generated only by a coupling of the Cu^{2+} centers within a dimer. The species responsible for the appearance of transitions within the triplet state are thought to be Cu(II) dimeric centers formed by aggregation of two $\{\text{CuCo}(\text{H}_2\text{L})(\text{L})_2\}$ fragments of **1–3** present in solution. The residual monomeric spectra in the $g \approx 2$ region are indicative of the existence of an equilibrium in solution between the dimeric and monomeric Cu(II) centers in aggregated and free $\{\text{CuCo}(\text{H}_2\text{L})(\text{L})_2\}$ fragments, respectively, with varying degrees of stability. The fragmentation process of **1–3** in solution was screened by electrospray ionization mass spectrometry.

Introduction

The design and construction of supramolecular assemblies of metals utilizing coordinate and noncovalent bonding motifs has become a topic of increasing interest in recent years, because of the fascinating structures and novel functionalities of such assemblies, such as the control of redox activity magnetic and luminescence properties, as well as anion recognition and electrochemical sensing.¹ The

creation of engineered molecular components for the assembly of electronic, photonic, and mechanical devices is the goal of nanotechnology.² Molecular self-assembly has

* Corresponding author. Tel.: +380 44 235 4371. Fax: +380 44 296 2467. E-mail: vassilyeva@univ.kiev.ua.

[†] National Taras Shevchenko University.

[‡] Universität Heidelberg.

[§] University of Western Australia.

^{||} University of Wrocław.

- (1) (a) See, for example: Slone, R. V.; Hupp, J. T.; Stern, C. L.; Albrecht-Schmitt, T. E. *Inorg. Chem.* **1996**, *35*, 4096–4097. (b) Würthner, F.; Sautter, A. *Chem. Commun.* **2000**, 445–446. (c) Lahav, M.; Gabai, R.; Shipway, A. N.; Willner, I. *Chem. Commun.* **1999**, 1937–1938. (d) Park, K.-M.; Kim, S.-Y.; Heo, J.; Whang, D.; Sakamoto, S.; Yamaguchi, K.; Kim, K. *J. Am. Chem. Soc.* **2002**, *124*, 2140–2147. (e) Roland, B. K.; Selby, H. D.; Carducci, M. D.; Zheng, Z. *J. Am. Chem. Soc.* **2002**, *124*, 3222–3223. (f) Murugesu, M.; Anson, C. E.; Powell, A. K. *Chem. Commun.* **2002**, 1054–1055. (g) Zhang, L.; Jones, R. A.; Lynch, V. M. *Chem. Commun.* **2002**, 2986–2987. (2) (a) Merkle, R. C. *Nanotechnology* **2000**, *11*, 89–99. (b) Swiegers, G. F.; Malefetse, T. J. *Chem. Rev.* **2000**, *100*, 3483–3538. (c) Swiegers, G. F.; Malefetse, T. J. *Coord. Chem. Rev.* **2002**, *225*, 91–121.

emerged as an attractive approach to the fabrication of new materials;³ this process involves the spontaneous aggregation of small molecular building blocks in solution that recognize each other through multiple molecular recognition sites to form supramolecules. Self-assembly by H-bonding is a very important process in the formation of biological architectures.⁴ In material sciences, this mechanism is being developed as an efficient design tool to control organizing individual molecular entities. It has recently been recognized that hydrogen bonds play a significant role in the transmission of ferromagnetic interactions in organic ferromagnets and in exchange coupling of transition metal ions.⁵ There have been many concepts and ideas to predict which species will self-assemble in solution,^{3,6} and these considerations are mainly based on the information stored in the building blocks, that is, the number of receptor groups, their positioning in space, the electronic configurations of the metal ions, and the specificity of molecular recognition.

The number of heteropolynuclear metal assemblies has increased enormously over the recent years; however, their "rational design" is still one of the major challenges for inorganic chemists, and exploratory syntheses, with the hope of discovering new materials with useful properties, have been a common alternative. A popular two-step approach for the synthesis of these species uses a preformed metal-containing ligand that is reacted with a second type of metal ion via the free coordination donors. We have developed a synthetic strategy that eliminates the separate step of building block construction: a metal-containing ligand can be formed from zerovalent metal and an appropriate ligand and subsequently self-assembles with a second metal center in the same reaction vessel.

In previous work, we have shown how heterometallic Cu^{II}/Co^{III} complexes can be prepared starting from zerovalent copper, cobalt(II) salt, and diethanolamine in nonaqueous solution at ambient conditions of air and water.⁷ Metallic copper readily dissolves under magnetic stirring while the reaction mixture is heated mildly. Compounds that feature heterotetranuclear cations of a puckered cyclic structure form as a result of the self-assembly of copper aminoalkoxo species generated in situ and cobalt complex anions self-organized in the reaction medium. The zerovalent copper and Co²⁺ ions in the initial reaction mixture are oxidized to Cu²⁺ and Co³⁺, respectively, by dioxygen from the air; the

amino alcohol, which forms alkoxo bridges, realizes its potential to coordinate in deprotonated form, and this probably helps to stabilize the products, formed without addition of external base.

Among metallosupramolecular structures studied, examples of those comprising three different metal atoms are limited to a small number of known and fully characterized complexes.⁸ Within the approach mentioned above, we proceeded to explore whether copper aminoalkoxo species could bind two different metals to result in the formation of thermodynamically favored heterotrimetallic arrays that optimally satisfy the requirements of different metal atoms. We describe here the synthesis, characterization, and magnetic properties in the solid state and solution of the series of heterotrimetallic complexes [Ni(H₂L)₂][CoCu(L)₂(H₂L)(NCS)]₂(NCS)₂ (**1**), [Ni(H₂L)₂][CuCo(L)₂(H₂L)(NCS)]₂·Br₂·2H₂O (**2**), and [CuCoCd(L)₂(H₂L)₂(NCS)]Br₂·CH₃OH (**3**) with diethanolamine (H₂L) as a bridging ligand prepared using zerovalent copper and two different metal salts as starting materials.

Experimental Section

General. Commercial reagents were used without further purification; all experiments were carried out under aerobic conditions. Elemental analyses were performed by atomic absorption spectroscopy for metals and by the Faculty of Chemistry, University of Wrocław, microanalytical service for C, H, and N. Infrared spectra were recorded on KBr pellets (4000–400 cm⁻¹) and in DMF (dimethylformamide) solutions (2300–1900 cm⁻¹) on a Bruker IFS 66/S FTIR spectrometer using conventional techniques. Electrospray mass spectra were measured on a Micromass/Waters Q-tof Ultima ESI mass spectrometer. Isotopic abundance patterns were calculated using the program that is freely available at the Sheffield University Web site: <http://www.shef.ac.uk/chemistry/chemputer/isotopes.html>. The EPR spectra were recorded on a Bruker ESP 300E spectrometer operating at X-band and equipped with a Bruker NMR gaussmeter ER 035M and a Hewlett-Packard microwave frequency counter HP 5350B. Magnetic susceptibility data of powdered samples of **1–3** were measured over the temperature range 4.5–300 K in the presence of a magnetic field between 0.1 and 5 T with a SQUID-based (Quantum Design) MPMSXL-5-type magnetometer. Magnetization data of powdered samples were measured at a magnetic field of 0.5 T. In all cases, diamagnetic corrections for the sample holders were applied to the data. Diamagnetic corrections for the samples were determined from Pascal's constants.

Synthesis of {[Ni(H₂L)₂][CoCu(L)₂(H₂L)(NCS)]₂(NCS)₂ (1**).** Copper powder (0.32 g, 5 mmol), Co(NCS)₂·2H₂O (1.06 g, 5 mmol), Ni(NCS)₂·2H₂O (0.52 g, 2.5 mmol), CH₃OH (15 mL), and diethanolamine (3.5 mL) were heated to 50–60 °C and stirred magnetically until total dissolution of the copper was observed (30–40 min). Dark green crystals suitable for X-ray crystallography were obtained from the dark green solution after 1 day. They were filtered off, washed with dry methanol, and finally dried in vacuo at room temperature. Yield: 2 g, 58% (per copper). IR (KBr, cm⁻¹):

- (3) Lehn, J. M. *Supramolecular Chemistry, Concepts and Perspectives*; VCH: Weinheim, Germany, 1995.
 (4) (a) Kricheldorf, M. J.; Lehn, J.-M. *Struct. Bonding (Berlin)* **2000**, *96*, 3–29 and references therein. (b) *Hydrogen Bonding in Biological Structures*; Jeffrey, G. A., Saenger, W., Eds.; Springer: Berlin, 1991. (c) Steiner, T. *Angew. Chem.* **2002**, *114*, 48–76.
 (5) (a) Romero, F. M.; Zissel, R.; Bonnet, M.; Pontillon, Y.; Ressouche, E.; Schweizer, J.; Delley, B.; Grand, A.; Paulsen, C. *J. Am. Chem. Soc.* **2000**, *122*, 1298–1309. (b) Desplanches, C.; Ruiz, E.; Rodriguez-Fortea, A.; Alvarez, S. *J. Am. Chem. Soc.* **2002**, *124*, 5197–5205. (c) Ali, M.; Ray, A.; Sheldrick, W. S.; Mayer-Figge, H.; Gao, S.; Sahmes, A. I. *New J. Chem.* **2004**, 412–417.
 (6) (a) Caulder, D. L.; Raymond, K. N. *Acc. Chem. Res.* **1999**, *32*, 975–982. (b) Navarro, J. A. R.; Lippert, B. *Coord. Chem. Rev.* **1999**, *185–186*, 653–667.
 (7) Makhankova, V. G.; Vassilyeva, O. Yu.; Kokozay, V. N.; Reedijk, J.; van Albada, G. A.; Jezierska, J.; Skelton, B. W. *Eur. J. Inorg. Chem.* **2002**, 2163–2169.

- (8) (a) Colacio, E.; Dominguez-Vera, J. M.; Ghazi, M.; Kivekäs, R.; Klinga, M.; Moreno, J. M. *Inorg. Chem.* **1998**, *37*, 3040–3045 and references therein. (b) Kou, H.-Z.; Zhou, B. C.; Wang, R.-J. *Inorg. Chem.* **2003**, *42*, 7658–7665. (c) Verani, C. N.; Rentschler, E.; Weyhermüller, T.; Bill, E.; Chaudhuri, P. *J. Chem. Soc., Dalton Trans.* **2000**, 251–258.

Table 1. Crystallographic Data and Relevant Data Referring to the Structures Solution and Refinement

parameter	1	2	3
chemical formula	C ₃₆ H ₈₀ Co ₂ Cu ₂ Ni ₂ Ni ₁ O ₁₆ S ₄	C ₃₄ H ₈₄ Br ₂ Co ₂ Cu ₂ Ni ₁₀ Ni ₁ O ₁₈ S ₂	C ₁₈ H ₄₄ Br ₂ Cd ₁ Co ₁ Cu ₁ N ₅ O ₉ S ₁
formula weight	1369.02	1448.69	901.34
space group	<i>P</i> 2 ₁ / <i>c</i>	<i>P</i> 2 ₁ / <i>c</i>	<i>Pca</i> 2 ₁
<i>a</i> (Å)	12.3328(9)	12.723(3)	17.709(2)
<i>b</i> (Å)	10.2011(8)	10.387(2)	11.0550(10)
<i>c</i> (Å)	22.653(2)	23.011(5)	15.941(2)
α (deg)	90	90	90
β (deg)	104.056(2)	105.769(4)	90
γ (deg)	90	90	90
<i>V</i> (Å ³)	2764.6(4)	2926.5(11)	3120.8(6)
<i>Z</i>	2	2	4
ρ _{calcd} (g/cm ³)	1.645	1.644	1.918
μ (mm ⁻¹)	1.902	3.092	4.554
<i>F</i> (000)	1424	1488	1796
θ _{min} , θ _{max} (deg)	1.7, 34.65	1.66, 25.0	1.84, 26.3
<i>T</i> (K)	150(2)	296(2)	150(2)
reflns collected	54368	14193	43030
reflns unique	11859	5125	3312
<i>R</i> _{int}	0.054	0.094	0.057
reflns observed [<i>F</i> > 4σ(<i>F</i>)]	8512	3016	2820
<i>R</i>	0.044	0.065	0.050
<i>R</i> _w	0.052	0.082	0.072
no. of variables	498	327	347
GoF	1.102	1.256	1.145

3451(sh), 3390(m), 3290(m), 3184(m), 2954(s), 2927(s), 2872(s), 2853(s), 2103(s), 2093(sh), 2045(s), 2039(sh), 2028(s), 2022(s), 1466(sh), 1455(s), 1377(m), 1354(m), 1246(w), 1219(w), 1194(w), 1165(w), 1152(w), 1108(m), 1082(sh), 1065(s), 1050(s), 1025(sh), 1008(sh), 990(m), 951(w), 923(w), 911(w), 885(w), 870(w), 816(w), 786(w), 750(w), 722(w), 694(w), 628(w), 607(m), 571(m), 555(w), 534(m), 490(w), 470(w), 459(w), 418(w). C₃₆H₈₀Co₂Cu₂Ni₂NiO₁₆S₄ (*M* = 1369.02): calcd Cu 9.28, Co 8.61, Ni 4.29, C 31.58, H 5.89, N 12.28; found Cu 8.8, Co 8.0, Ni 3.9, C 31.56, H 5.92, N 12.05%.

Synthesis of {[Ni(H₂L)₂][CuCo(L)₂(H₂L)(NCS)]₂·Br₂·2H₂O (2). This complex was obtained similarly to **1**, with Ni(NCS)₂·2H₂O replaced by NiBr₂·2H₂O (0.64 g, 2.5 mmol). Yield: 2.77 g, 76% (per copper). IR (KBr, cm⁻¹): 3499(sh), 3451(m), 3405(m), 3280(m), 3202(m), 3169(m), 3098(m), 2954(s), 2924(s), 2870(sh), 2855(s), 2728(w), 2709(w), 2673(w), 2463(br), 2107(sh), 2088(s), 1905(br), 1850(sh), 1630(w), 1618(w), 1506(sh), 1456(s), 1422(sh), 1377(m), 1360(m), 1348(m), 1330(sh), 1309(sh), 1283(w), 1268(w), 1248(w), 1223(w), 1180(w), 1149(w), 1109(m), 1084(sh), 1063(s), 1049(sh), 1022(m), 1006(sh), 992(m), 963(sh), 912(m), 884(w), 874(w), 817(w), 788(w), 721(w), 696(w), 629(w), 606(m), 574(m), 562(sh), 537(m), 519(m), 496(w), 472(w), 459(w), 447(w), 420(w). C₃₄H₈₄Br₂Co₂Cu₂Ni₁₀Ni₁O₁₈S₂ (*M* = 1448.69): calcd Cu 8.77, Co 8.14, Ni 4.05, C 28.19, H 5.84, N 9.67; found Cu 8.3, Co 8.1, Ni 3.9, C 28.51, H 5.83, N 9.86%.

Synthesis of [CuCoCd(L)₂(H₂L)₂(NCS)Br₂]·CH₃OH (3). Copper powder (0.16 g, 2.5 mmol), Co(NCS)₂·2H₂O (0.53 g, 2.5 mmol), CdBr₂·4H₂O (0.86 g, 2.5 mmol), CH₃OH (20 mL), and diethanolamine (2 mL) were heated to 50–60 °C and stirred magnetically until total dissolution of copper was observed (1 h). Dark green crystals suitable for X-ray crystallography were deposited in several days after successive addition of PrⁱOH into the resulting green solution. The crystals were filtered off, washed with dry methanol, and finally dried in vacuo at room temperature. Yield: 0.7 g, 31% (per copper). IR (KBr, cm⁻¹): 3453(m), 3290(w), 3210(m), 3165(m), 2954(s), 2924(s), 2872(sh), 2857(s), 2091(s), 1624(w), 1496(sh), 1460(s), 1389(sh), 1387(m), 1342(m), 1291(w), 1271(w), 1243(w), 1219(w), 1201(w), 1154(w), 1107(sh), 1090(sh), 1064(s), 1048(s), 1011(m), 984(sh), 915(w), 878(w), 867(w), 841(w), 818(w), 784(w), 721(w), 700(w), 638(m), 616(w), 603(sh), 572-

(m), 552(m), 516(w), 497(w), 478(w), 450(w). C₁₈H₄₄Br₂Cd₁Co₁Cu₁N₅O₉S₁ (*M* = 901.34): calcd Cu 7.05, Co 6.54, Cd 12.47, C 23.99, H 4.92, N 7.77; found Cu 7.1, Co 6.5, Cd 12.3, C 24.12, H 4.97, N 7.56%.

The compounds are soluble in DMF and sparingly soluble in methanol and CH₃CN. All of the complexes are indefinitely stable in air.

X-ray Crystallographic Analysis. Details of the data collection and processing, structure analysis, and refinement are summarized in Table 1. Diffraction experiments were performed on a Bruker SMART CCD area-detector diffractometer (*ω* rotation scans with narrow frames) equipped with graphite-monochromated Mo Kα radiation (*λ* = 0.71073 Å). The data were corrected for Lorentz-polarization effects and for the effects of absorption (multiscan method using SADABS⁹). The structures were solved by direct methods and refined by full-matrix least-squares methods on *F* using the XTAL 3.7 program.¹⁰ The assignment of each of the metal atoms is based on refinement and on comparison of the bond lengths with the literature values. The Cu/Co/Ni and Cu/Co/Cd ratios obtained are in agreement with those found from analysis. In general, the non-hydrogen atoms were refined anisotropically.

One oxygen atom of one diethanolamine ligand in **1** was found to be disordered over two sites, O(37) and O(37'), each assigned populations of 0.5 after trial refinement. All hydrogen atoms were located and refined except for those associated with the disordered part of this diethanolamine ligand, which were located in the difference map [H(37) and H(37')] or calculated [H(36a,b), H(36'a,b)]. The thiocyanate group [C(01), S(01)] was modeled as being disordered, the populations of the two components refining to 0.905(2) and 1 – 0.905(2). In **2**, a model was chosen with a disordered bromine [Br(1') population is 1–0.869(4)] plus an associated water molecule [O(01), population 0.869(4)]. The minor component of the water molecule was not located. The oxygen atom O(37) is, as in **1**, disordered over two sites (each with population 0.5 after initial trial refinement). The thiocyanate group [N(01),

(9) Sheldrick, G. M. *SADABS: Program for Empirical Absorption Correction of Area Detector Data*. University of Göttingen: Göttingen, Germany, 1996.

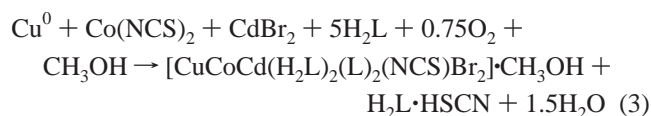
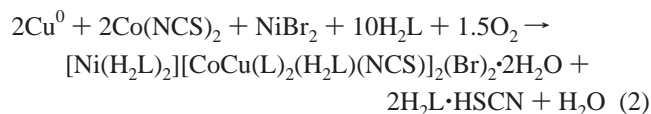
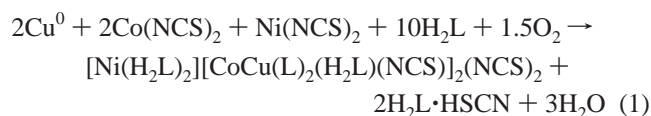
(10) Hall, S. R.; du Boulay, D. J.; Olthof-Hazekamp, R. *XTAL 3.7 System*; University of Western Australia, Western Australia, Australia, 2000.

C(O1), S(O1)] is, as in **1**, also disordered over two sites, but the site occupancy factors are now equal after initial trial refinement. H atoms of solvent water molecule and on the disordered O(37) and O(37') atoms were not located. The atoms of the thiocyanate group were refined with isotropic displacement parameters. The C and S atoms of the thiocyanate group in **3** and the NHCH₂CH₂OH of the uncoordinated chain [N(4), C(15), C(16), O(8)] of the diethanolamine ligand on the Cd atom are disordered over two sites, all with population 0.5 after initial trial refinement. As might be expected from this disorder, as well as from the presence of heavy atoms such as Br and Cd, some hydrogen atoms were not located, but it would seem likely that the ligand O atoms are deprotonated when bridging between two metal sites. The other H atoms on the OH groups have been assigned as well as possible. The geometry of the thiocyanate group was not satisfactory, so the bond lengths and angle of the thiocyanate group were restrained to ideal values. Despite the large ellipsoids for the methanol solvent molecule [O(0)], a disordered model could not be found; the OH hydrogen atom was not located.

All bond distances and angles within diethanolamine and thiocyanate ligands are as expected.

Results and Discussion

Synthesis. The copper powder and solid metal salts were taken in the molar ratios of Cu/Co/Ni = 2:2:1 and Cu/Co/Cd = 1:1:1 in methanol, and diethanolamine was then added. The reaction was initiated and brought to completion by heating and stirring. Green solutions were obtained at the end of the reaction that afforded dark green microcrystals of the heterotrimetallic complexes directly (**1**, **2**) or upon successive addition of PrⁱOH (**3**). Their formation can be understood if one considers the following reaction schemes:



Interestingly, in the presence of the third metal ion (Ni, Cd), dissolution of copper is 2–3 times faster compared to the reaction progress in Cu–CoX₂–H₂L–O₂–Solv systems.⁷ The compounds can be recrystallized from methanol in relatively low yield.

The IR spectroscopic investigations of the title compounds in the range 4000–400 cm⁻¹ showed all the characteristic ligand peaks. The presence of hydroxo groups and solvents (water, methanol) can be clearly observed in the spectra [bands at 3451, 3390 (**1**); 3451, 3405, 1630 (**2**); 3453 (**3**) cm⁻¹]. In addition, the ν(CN) stretching is detected in the 2100–2000 cm⁻¹ region (Figure 1). The frequencies of the observed bands (ca. 2090 cm⁻¹) suggest a terminal N-bonded thiocyanate. The complicated pattern of the spectrum of **1**

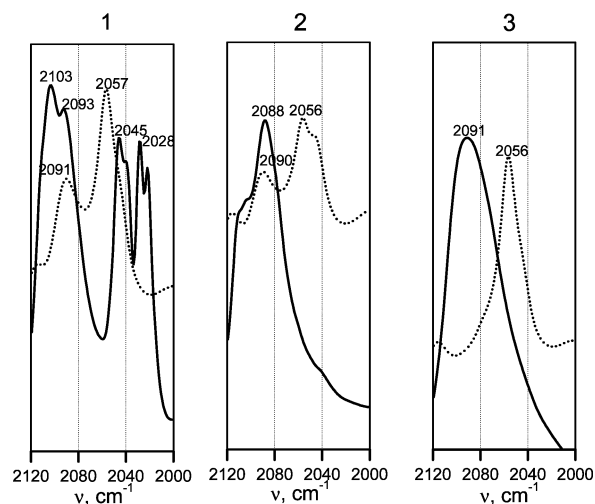


Figure 1. Fragments of the IR spectra of **1–3** in the solid state (—) and DMF solutions (···).

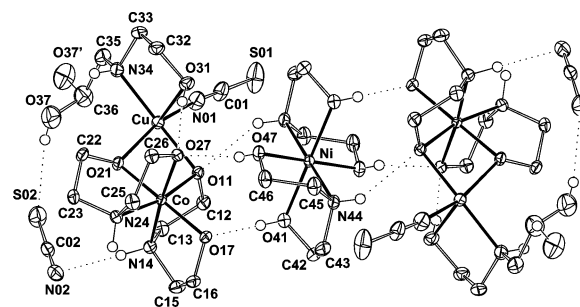


Figure 2. Structure of the pentanuclear aggregate {[Ni(H₂L)₂][CoCu(L)₂(H₂L)(NCS)]₂}²⁺ in **1** and **2** with the numbering scheme (H atoms are omitted for clarity, non-hydrogen atoms are shown as 50% thermal ellipsoids, and only one of the two sets of disordered atoms of the NCS⁻ group is shown).

indicates the presence of both coordinated and uncoordinated NCS⁻ groups (supported by the X-ray structural study), although the possibility of anion exchange in a KBr disk and pressure-induced changes cannot be ruled out. The ν(CN) bands shift to lower frequencies when the compounds are dissolved in DMF (Figure 1), which provides clear evidence of the appearance of uncoordinated NCS⁻ groups in solution.

Taking into account the reaction conditions and results of elemental analyses and given the hydrogen bonding in the lattice as well as the unambiguous valence state assignments for the metal ions (see below), the formulas as given in **1–3** can be deduced. The assumption of neutral and doubly deprotonated amino alcohols that follows from counting the electrostatic charges was verified structurally.

Crystal Structures 1 and 2. The overall structural configurations of isomorphous **1** and **2** are similar with the uncoordinated NCS⁻ group in **1** replaced by disordered Br⁻ anion and water molecule in **2**. The molecular diagram and numbering scheme of **1** is shown in Figure 2, which illustrates the general geometry of the two compounds. The most prominent feature of the structures of **1** and **2** is the formation of the “pentanuclear” aggregate {[Ni(H₂L)₂][CoCu(L)₂(H₂L)(NCS)]₂}²⁺ made up of two neutral [CoCu(L)₂(H₂L)(NCS)] units and the previously unknown cation [Ni(H₂L)₂]²⁺. The Ni cation is on a crystallographic inversion

Table 2. Selected Bond Lengths (Å) and Angles (deg) for **1** and **2**

	1	2
Cu...Co	2.9256(5)	2.923(2)
Co...Ni	4.6626(4)	4.640(1)
Cu...Ni	5.2727(4)	5.328(1)
Cu–O(11)	1.9880(15)	1.991(5)
Cu–O(21)	1.9736(17)	1.973(7)
Cu–O(31)	2.2436(18)	2.255(8)
Cu–N(34)	2.0276(19)	2.031(8)
Cu–N(01)	1.958(3)	2.05(3)
Cu–N(01')		1.94(2)
Co–O(11)	1.9271(17)	1.926(7)
Co–N(14)	1.949(2)	1.948(9)
Co–O(17)	1.8959(15)	1.900(6)
Co–O(21)	1.8987(15)	1.889(6)
Co–N(24)	1.950(2)	1.936(8)
Co–O(27)	1.9201(15)	1.924(6)
Ni–O(41)	2.0995(18)	2.085(7)
Ni–N(44)	2.060(2)	2.064(8)
Ni–O(47)	2.0651(16)	2.071(6)
O(11)–Cu–O(21)	78.22(6)	78.2(2)
O(11)–Cu–O(31)	90.70(6)	91.0(2)
O(11)–Cu–N(34)	171.07(8)	169.8(4)
O(11)–Cu–N(01)	92.62(8)	91.4(6)
O(11)–Cu–N(01')		93.8(6)
O(21)–Cu–O(31)	102.10(7)	101.8(3)
O(21)–Cu–N(34)	98.15(8)	97.2(3)
O(21)–Cu–N(01)	157.65(9)	151.4(7)
O(21)–Cu–N(01')		165.4(6)
O(31)–Cu–N(34)	82.04(7)	81.0(4)
O(31)–Cu–N(01)	98.32(9)	105.0(7)
O(31)–Cu–N(01')		90.4(6)
N(34)–Cu–N(01)	93.56(9)	96.8(6)
N(34)–Cu–N(01')		92.6(6)
O(11)–Co–N(14)	87.24(8)	87.3(3)
O(11)–Co–O(17)	95.95(7)	96.0(3)
O(11)–Co–O(21)	81.56(7)	81.9(3)
O(11)–Co–N(24)	168.46(7)	168.4(3)
O(11)–Co–O(27)	91.26(7)	90.8(3)
N(14)–Co–O(17)	85.79(7)	85.2(3)
N(14)–Co–O(21)	91.31(7)	91.5(3)
N(14)–Co–N(24)	96.64(8)	97.1(4)
N(14)–Co–O(27)	175.06(7)	175.1(3)
O(17)–Co–O(21)	176.28(7)	176.2(3)
O(17)–Co–N(24)	95.18(7)	95.1(3)
O(17)–Co–O(27)	89.68(7)	90.5(3)
O(21)–Co–N(24)	87.47(7)	87.2(3)
O(21)–Co–O(27)	93.13(6)	92.7(3)
N(24)–Co–O(27)	85.73(7)	85.6(3)
O(41)–Ni–N(44)	82.78(8)	83.4(3)
O(41)–Ni–O(47)	94.51(7)	94.5(3)
N(44)–Ni–O(47)	82.28(7)	82.4(3)

center, and the Cu/Co moieties are situated on general positions. The presence of the molecular inversion center requires all five metal atoms to lie in the same plane. In the Cu–Co–Cu–Co parallelogram centered on Ni, the bridged Cu...Co separations are approximately 2.924 Å, and the other metal–metal distances vary from 4.640(1) to 5.328(1) Å (Table 2). An idea of the size of this assembly is given by the distance of 17.592(7) Å, **1**, and 17.641(2), **2**, between the uncoordinated hydroxo O atoms of the H₂L ligands [O(37)] located at opposite edges.

The divalent nickel ion adopts a slightly distorted octahedral environment by interacting with two oxygen and two nitrogen atoms in the equatorial plane and two axially disposed oxygen atoms O(41) and O(41){1-x, 1-y, 1-z} from two H₂L ligands (average 2.074 Å); the cis bond angles around Ni range from 82.28(7)° to 97.73(7)°; the trans bond angles are equal to 180° (Table 2).

The metal atoms within the [CoCu(L)₂(H₂L)(NCS)] units are bridged by two oxygen atoms of two diethanolamine ligands. The Cu and Co atoms deviate from the least-squares plane through the Co, Cu, O(11), O(21) atoms [Co, Co 0.081(1), 0.087(1) (**1**) and 0.013(2), 0.011(2) (**2**)] in the direction of O(27) and O(31) with the O(11), O(21) atoms displaced by 0.204(2), 0.221(2) Å (**1**) and 0.267(8), 0.278(8) Å (**2**) in the other direction, toward N(14) and O(37').

The copper(II) atom has distorted square-pyramidal coordination to a NO₃N_{NCS} donor set [in the case of **2**, the copper atom also makes a weak contact to one site of disordered O(37) atom at 2.74(3) Å]. The four copper–ligand bonds in the plane vary from 1.94(2) and 2.031(8) Å, while the axial bond to oxygen atom O(31) of the H₂L ligand is elongated (average 2.250 Å, Table 2). This long distance also confirms the identification of the protonated function of the O(31) oxygen atom. The geometry at the cobalt ion is almost octahedral, with Co–O(N) distances in the range 1.889(6)–1.950(2) Å; the cis bond angles around Co range from 81.56(7)° to 97.1(4)°, and the trans bond angles range from 168.4(3)° to 176.28(7)° (Table 2), similar to those of low-spin cobalt(III) in an octahedral environment.¹¹ A strong intramolecular hydrogen bond from the OH group of the neutral diethanolamine ligand on the copper atom, O(31), to the oxygen atom O(27) of L on the Co center is present (Table 3).

Each [CoCu(L)₂(H₂L)(NCS)] unit is linked to the central Ni complex by two strong O–H...O[−] and one weaker N–H...O[−] charge-assisted hydrogen bonds, this arrangement producing eight-membered H-bonded rings (Figure 2, Table 3). Additional intermolecular association in the lattice occurs through the hydrogen bonding of the N–H...N, N–H...S, O–H...S, and N–H...Br types involving thiocyanate groups (**1**) and bromide anions (**2**) to form 3D frameworks (Table 3).

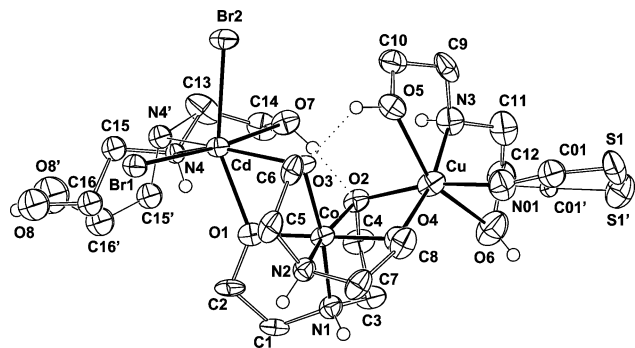
Crystal Structure of 3. X-ray crystallographic analysis of **3** reveals an asymmetric three-metal-atom core with metal atoms in a triangular array (Figure 3, Table 4). With Cd²⁺ instead of Ni²⁺, a different structure is obtained: the [CoCu(L)₂(H₂L)(NCS)] unit is now linked to the Cd center through coordination of oxygen atoms of L groups on the Co atom to form a discrete heterotrimetallic molecular species. The structural properties of the Cu/Co moiety are similar to those in **1** and **2**, with the Co atom being six-coordinate [Co–O(N) distances in the range 1.873(11)–1.948(9) Å, cis bond angles around Co in the range from 81.8(4)° to 99.7(5)°, trans bond angles in the range from 167.8(5)° to 173.3(5)°] and the Cu atom displaying a distorted square-pyramidal coordination [Cu–O(N) distances in the plane vary from 1.891(14) to 2.064(10) Å, and the axial bond to O(5) is 2.370(11) Å] (Table 4). In addition, Cu is weakly bonded to oxygen atom O(6) at 2.83(2) Å. The geometry of the cadmium atom can be described as distorted octahedral with donor atoms of diethanolamine ligands and bromine atom,

(11) Wells, A. F. *Structural Inorganic Chemistry*, 5th ed.; Clarendon Press: Oxford, U.K., 1986.

Table 3. Hydrogen Bonding Distances (Å) and Angles (deg) for Complexes **1** and **2**^a

	1	2
O(31)···O(27)	2.560(2)	2.57(1)
H(31)···O(27)	1.80(4)	1.822(6)
O(31)–H(31)···O(27)	158(3)	134.6(4)
O(41)···O(17)	2.584(2)	2.540(9)
H(41)···O(17)	1.78(4)	1.623(6)
O(41)–H(41)···O(17)	174(4)	166.6(5)
O(47)···O(27)	2.558(2)	2.541(8)
H(47)···O(27)	1.93(3)	1.678(5)
O(47)–H(47)···O(27)	166(4)	155.3(4)
N(44)···O(11 ¹)	3.106(3)	3.09(1)
H(44)···O(11 ¹)	2.39(3)	2.216(7)
N(44)–H(44)···O(11 ¹)	148(3)	151.9(5)
N(14)···X	3.004(3) [X = N(02)]	3.283(9) [X = Br(1)]
H(14)···X	2.13(3)	2.308(1)
N(14)–H(14)···X	156(3)	164.3(5)
N(24)···X ²	3.048(3) [X = N(02)]	3.321(8) [X = Br(1)]
H(24)···X ²	2.24(3)	2.541(1)
N(24)–H(24)···X ²	147(3)	141.3(5)
N(34)···X ³	3.462(2) [X = S(02)]	3.22(2) [X = Br(1 ¹)]
H(34)···X ³	2.74(3)	2.34(1)
N(34)–H(34)···X ³	152(3)	132.5(6)
O(37)···S(02)	3.121(5)	–
H(37)···S(02)	2.353(–)	–
O(37)–H(37)···S(02)	150.9(–)	–
O(37 ¹)···S(01 ⁴)	3.323(5)	–
H(37 ¹)···S(01)	2.421(–)	–
O(37 ¹)–H(37 ¹)···S(01)	149.1(–)	–
O(37 ²)···X	3.06(1) [X = S(01 ⁴)]	3.11(3) [X = Br(1 ¹)]
H(37 ²)···X	2.071(–)	–
O(37 ²)–H(37 ²)···X	168.4(–)	–
O(01)···Br(1)	–	3.29(3)

^a Symmetry transformations used to generate equivalent atoms: (1) $1 - x, 1 - y, 1 - z$; (2) $-x, -y, 1 - z$; (3) $-x, 1/2 + y, 1/2 - z$; (4) $1 - x, y - 1/2, 1/2 - z$.

**Figure 3.** Molecular structure of **3** with the numbering scheme (H atoms are omitted for clarity, and non-hydrogen atoms are shown as 30% thermal ellipsoids).

Br(2), in the equatorial plane and the apical positions occupied by oxygen O(7) and another bromine atom. The O(7)–Cd–Br(1) angle is nearly linear at 173.3(3)°.

The CH₂OH groups of the neutral diethanolamine ligands form strong intramolecular hydrogen bonds with the CH₂O[–] groups of the ligands on the Co center, as evidenced by the O(5)···O(3) and O(7)···O(2) distances and the O–H···O angles (Table 5, Figure 3). A further hydrogen-bonding interactions between heterotrinuclear molecules [O(8), O(8')···O(5){*x, y - 1, z*}] link them into a 3D framework. The methanol molecule is at distances consistent with the

Table 4. Selected Bond Distances (Å) and Angles (deg) for **3**

Cu···Co	2.967(3)	Co···Cd	3.323(2)
Cu···Cd	5.201(2)		
Cd–Br(1)	2.7058(16)	Co–O(4)	1.873(11)
Cd–Br(2)	2.6636(17)	Co–N(1)	1.940(12)
Cd–O(1)	2.265(12)	Co–N(2)	1.942(12)
Cd–O(3)	2.402(10)	Cu–O(2)	2.064(10)
Cd–O(7)	2.444(10)	Cu–O(4)	1.966(11)
Cd–N(4)	2.37(2)	Cu–O(5)	2.370(11)
Cd–N(4')	2.40(3)	Cu–O(6)	2.829(15)
Co–O(1)	1.877(10)	Cu–N(3)	2.041(14)
Co–O(2)	1.948(9)	Cu–N(01)	1.891(14)
Co–O(3)	1.937(10)		
Br(1)–Cd–Br(2)	92.42(5)	O(2)–Co–O(3)	92.3(4)
Br(1)–Cd–O(1)	102.3(2)	O(2)–Co–O(4)	81.8(4)
Br(1)–Cd–O(3)	105.5(2)	O(2)–Co–N(1)	87.7(5)
Br(1)–Cd–O(7)	173.3(3)	O(2)–Co–N(2)	167.8(5)
Br(1)–Cd–N(4)	105.2(5)	O(3)–Co–O(4)	98.1(5)
Br(1)–Cd–N(4')	97.0(6)	O(3)–Co–N(1)	170.8(5)
Br(2)–Cd–O(1)	155.8(2)	O(3)–Co–N(2)	86.9(5)
Br(2)–Cd–O(3)	90.4(2)	O(4)–Co–N(1)	91.0(5)
Br(2)–Cd–O(7)	84.4(3)	O(4)–Co–N(2)	86.2(5)
Br(2)–Cd–N(4)	107.6(7)	N(1)–Co–N(2)	95.0(5)
Br(2)–Cd–N(4')	97.4(7)	O(2)–Cu–O(4)	76.8(4)
O(1)–Cd–O(3)	67.3(3)	O(2)–Cu–O(5)	91.6(4)
O(1)–Cd–O(7)	82.7(4)	O(2)–Cu–O(6)	91.7(4)
O(1)–Cd–N(4)	87.2(7)	O(2)–Cu–N(3)	93.0(5)
O(1)–Cd–N(4')	99.8(8)	O(2)–Cu–N(01)	167.6(6)
O(3)–Cd–O(7)	80.4(3)	O(4)–Cu–O(5)	93.5(4)
O(3)–Cd–N(4)	143.4(6)	O(4)–Cu–O(6)	115.4(5)
O(3)–Cd–N(4')	155.8(7)	O(4)–Cu–N(3)	167.8(5)
O(7)–Cd–N(4)	70.4(6)	O(4)–Cu–N(01)	95.5(6)
O(7)–Cd–N(4')	77.6(7)	O(5)–Cu–O(6)	150.9(4)
O(1)–Co–O(2)	92.3(4)	O(5)–Cu–N(3)	80.2(5)
O(1)–Co–O(3)	85.5(5)	O(5)–Cu–N(01)	98.7(6)
O(1)–Co–O(4)	173.3(5)	O(6)–Cu–N(3)	70.8(5)
O(1)–Co–N(1)	85.3(5)	O(6)–Cu–N(01)	82.8(6)
O(1)–Co–N(2)	99.7(5)	N(3)–Cu–N(01)	95.7(6)

Table 5. Hydrogen Bonding Distances (Å) and Angles (deg) for Complex **3**^a

O(5)···O(3)	2.57(1)
H(5)···O(3)	1.88(1)
O(5)–H(5)···O(3)	128.2(7)
O(7)···O(2)	2.60(2)
H(7)···O(2)	1.70(1)
O(7)–H(7)···O(2)	171.4(7)
O(8)···O(5 ¹)	2.68(4)
H(8)···O(5 ¹)	1.81(1)
O(8)–H(8)···O(5 ¹)	161(2)
O(8')···O(5 ¹)	2.72(5)
O(0)···O(8)	2.62(7)
O(0')···O(8')	2.86(8)
N(2)···Br(2 ²)	3.45(1)
H(2)···Br(2 ²)	2.524(2)
N(2)–H(2)···Br(2 ²)	166.3(7)

^a Symmetry transformations used to generate equivalent atoms: (1) $x, y - 1, z$; (2) $-x, -y, 1/2 + z$.

formation of hydrogen bonds to disordered hydroxo functions of H₂L ligand on the cadmium center (Table 5).

Magnetic Properties. Experimental magnetic data for **1–3** are displayed in Figure 4 as μ_{eff} vs T plots. These plots show that, in all cases, the magnetic behavior is paramagnetic. On the assumption that the Co^{III} ions are diamagnetic, the room-temperature magnetic moment for **3**, 1.95 μ_{B} , is typical for isolated $S = 1/2$ ions. The μ_{eff} values (per mole of complex) of the {Cu₂Co₂Ni} complexes **1** and **2** are 4.18 and 4.3 μ_{B} , respectively. These values are similar to the calculated value

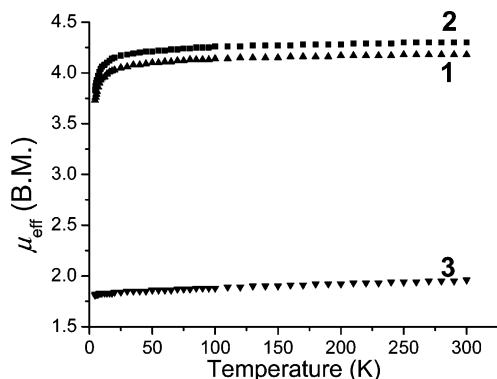


Figure 4. Plots of the effective magnetic moment vs temperature for 1–3.

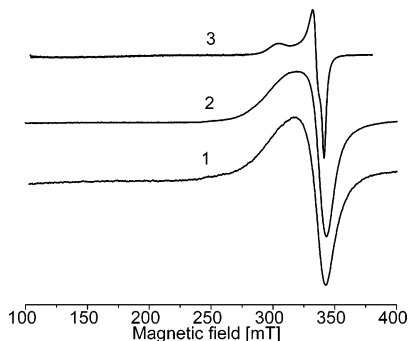


Figure 5. X-band EPR spectra of polycrystalline complexes of 1–3 measured at 295 K.

of $4.03 \mu_B$ for a high-spin $\text{Cu}_2^{\text{II}}\text{Ni}^{\text{II}}$ combination in which the constituent metals have typical μ_{eff} values of 1.9 and $3.0 \mu_B$.

The polycrystalline EPR spectra of 1–3 were measured at room and liquid nitrogen temperatures, and there is no significant variation with the temperature (Figure 5). At both temperatures, the spectra of 1 and 2 exhibit one anisotropic line with g_{\parallel} and g_{\perp} of about 2.3 and 2.05, respectively, a pattern that is typical for a square or elongated octahedral geometry with an unpaired electron located in the $d_{x^2-y^2}$ orbital. The g_{\parallel} part is broader, indicating hyperfine coupling that is not resolved. The polycrystalline EPR spectrum of 3 (295 and 77 K) appears to be due to rhombic geometry ($g_z = 2.304$, $g_y = 2.098$, $g_x = 2.050$) and differs from the typical axial spectra of 1 and 2 by higher anisotropy. The fine structure signals due to transitions within the spin-triplet state could not be found at either temperature.

A striking feature of the EPR spectra of 1–3 in frozen DMF and methanol (77 K) is the characteristics of a dimeric copper(II) triplet state (Figure 6). The hyperfine structure from the two coupled Cu^{II} centers is clearly observed for the $\Delta M_S = 1$ and $\Delta M_S = 2$ transitions. Careful examination of the spectra reveals two sets of fine structural parameters, suggesting the presence of two kinds of triplet-state species (with different zero-field splitting parameters) whose contributions depend on the parent compound and solvent used (Figure 6). The spectral patterns appear to be time- and concentration-dependent (a few representative spectra are shown in Figure 7, and the intensity is not scaled). The spectra of very fresh solutions (77 K) are dominated by the signals due to monomeric copper species and, in addition, a

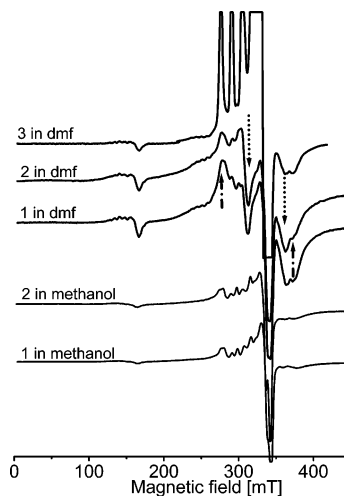


Figure 6. X-band EPR spectra of frozen solutions of 1–3 in DMF and methanol at 77 K. The arrows show signals due to $\Delta M_S = 1$ transitions of “perpendicular” orientation assigned to different triplet-state species present in the DMF solutions.

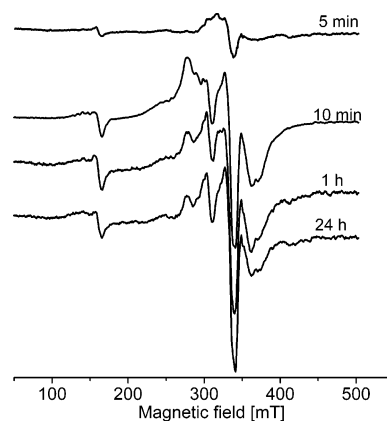


Figure 7. Representative time-dependent X-band EPR spectra of saturated DMF solution of 2 at 77 K.

half-field signal detected at 160 mT. The weak fine-structure signals originating from triplet-state transitions undergo a pronounced increase in intensity and resolution during 10–20 min. After the first few hours, the spectral features remain largely unchanged for a few days, although the relative intensities of the signals associated with different triplet-state species vary. There is a sharp difference in the relative intensities of the triplet-state lines and signals due to paramagnetic species in the case of 3. The former signals in frozen DMF solutions are about 10 times weaker and remain unchanged within a few days, suggesting that only a minor fraction of the copper(II) is in the coupled state.

The triplet EPR spectra are described by a spin Hamiltonian of the form¹²

$$\mathbf{H} = \mu_B \mathbf{B} \{ \mathbf{g} \} \mathbf{S} + \mathbf{I} \{ \mathbf{A} \} \mathbf{S} + D [S_z^2 - \frac{1}{3} S(S+1)] + E (S_x^2 - S_y^2) \quad (4)$$

The experimental spectra were fit with nonparallel \mathbf{g} and \mathbf{D} tensors through a computer simulation procedure as described

(12) Abragam, A.; Bleaney, B. *Electron Paramagnetic Resonance of Transition Ions*; Clarendon Press: Oxford, U.K., 1970.

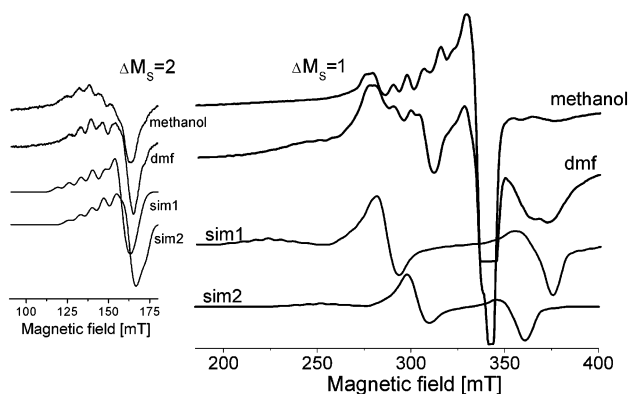


Figure 8. EPR spectra of frozen solutions of **1** in DMF and methanol (77 K); sim1 and sim2 are the theoretical spectra calculated using parameters reported in the text.

in ref 13. The main features of the frozen solution (methanol, DMF) spectra of compounds **1–3** were well simulated using two sets of spin-Hamiltonian parameters (see Figure 8 for a representative example): sim1 $g_z = 2.215$, $g_x = 2.067$, $g_y = 2.067$, $A_z = 0.0070$, $A_x = 0.0010$, $A_y = 0.0010 \text{ cm}^{-1}$, $D = 0.0790 \text{ cm}^{-1}$ and an angle (α) between the g_{zz} and D_{zz} directions of $30(1)^\circ$; sim2 $g_z = 2.256$, $g_x = 2.055$, $g_y = 2.056$, $A_z = 0.0070$, $A_x = 0.0010$, $A_y = 0.0010 \text{ cm}^{-1}$, $D = 0.0540 \text{ cm}^{-1}$, and $\alpha = 25(1)^\circ$.

These results clearly indicate the presence of a new species in solution originating from components of **1–3**. The triplets observed can be generated only by a coupling of the Cu^{2+} centers within a dimer. The EPR frozen solution spectra of **1–3** closely resemble the corresponding spectra of $[\text{Cu}_2\text{Co}_2(\text{H}_2\text{L})_2(\text{L})_4]\text{X}_2(\text{Solv})_n$ ($\text{X} = \text{Cl}, \text{Br}, \text{SCN}, \text{O}_2\text{CMe}, \text{I}$; $\text{Solv} = \text{H}_2\text{O}$ or/and $\text{CH}_3\text{OH}, \text{DMF}$; $n = 1–4$) complexes for which the tetranuclear cations are preserved in solution and magnetic dipole–dipole coupling between the copper(II) ions is maintained.⁷ Hence, the species responsible for the appearance of transitions within the triplet state are thought to be Cu(II) dimeric centers formed by aggregation of two $\{\text{CuCo}(\text{H}_2\text{L})(\text{L})_2\}$ fragments of **1–3** present in solution. The residual monomeric spectra in the $g \approx 2$ region are indicative of the existence of an equilibrium in solution between the dimeric and monomeric Cu(II) centers in aggregated and free $\{\text{CuCo}(\text{H}_2\text{L})(\text{L})_2\}$ fragments, respectively, with varying degrees of stability.

Mass Spectrometry. Electrospray ionization mass spectroscopy was used as a convenient solution-based technique to examine the behavior of the heterotrimetallic complexes in solution with the primary aim of screening possible transformation processes in these systems and detecting any novel species formed. Considerable effort was put into optimizing the solvent medium as the spectral patterns showed clear dependence on the solvent used, and eventually, a $\text{CH}_3\text{OH}/\text{DMF}$ mixture was chosen to make the results comparable to those obtained in the EPR studies. The ESI-

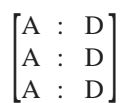
MS data in the positive ion mode revealed numerous singly and doubly charged species of molecular weights between m/z 189 and 1283. The random nature and number of peaks suggests decomposition of the compounds under the conditions used for these experiments; however, practical assignment of the most important peaks was straightforward. Surprisingly, the stability of the selective triple-hydrogen-bonded interaction in **1** and **2** appeared strong enough that the pentanuclear aggregate and its daughter fragments were observed in the ES mass spectra of the fresh solutions of the compounds. A number of peaks were assigned to the following species: $[\mathbf{1} - 2\text{NCS} - \text{H}_2\text{L} - 4\text{H} + \text{DMF}]^{2+}$ at m/z 609, $[\mathbf{1} - 3\text{NCS} - 4\text{H}]^{2+}$ at m/z 596, $[\mathbf{2} - 2\text{Br} - 2\text{H}_2\text{O} - \text{H} + \text{CH}_3\text{OH}]^+$ at m/z 1283, $[\mathbf{2} - 2\text{Br} - 2\text{H}_2\text{O} - \text{H}]^+$ at m/z 1251, $[\mathbf{2} - 2\text{Br} - 5\text{H}]^{2+}$ at m/z 642, $[\mathbf{2} - 2\text{Br} - 2\text{H}_2\text{O} - 5\text{H}]^{2+}$ at m/z 624 (peak masses quoted for ^{63}Cu ; the isotopic patterns were consistent with the given formulations). Further fragmentation of the heterotrimetallic complexes and exchange with the solvents used results in the formation of smaller species of varying stoichiometries observed in the spectra of both the solutions of **1** and **2** and those maintained at room temperature for several hours: $[\text{CuCo}(\text{HL})_3 + \text{DMF}]^+$ at m/z 508, $[\text{Co}_2\text{L}_3]^+$ at m/z 428, $[\text{CuCo}(\text{H}_2\text{L})_3(\text{HL}) + \text{DMF}]^{2+}$ at m/z 308, $[\text{Co}(\text{L}) + \text{NCS} + \text{DMF}]^+$ at m/z 293. The spectrum of **3** also exhibited an appreciably intense parent ion peak at m/z 450 ($[\mathbf{3} - 4\text{H}]^{2+}$). An interesting feature of the mass spectrum of **3** is the formation of CuCd species that result from fragmentation and reassembly of the complex: $[\text{CuCd}(\text{H}_2\text{L})(\text{L})_2(\text{NCS})\text{Br}]^+$ at m/z 625 and $[\text{CuCd}(\text{H}_2\text{L})(\text{L})(\text{NCS})\text{Br}]^+$ at m/z 522. This high-energy process indicates that the formation of such molecules from the components of the heterotrimetallic complexes in solution might be practical. Indeed, in the spectrum of **1**, we observed a low-intensity peak at m/z 819 that was tentatively assigned to the $[\text{Cu}_2\text{Co}_2(\text{H}_2\text{L})(\text{L})_4(\text{NCS})]^+$ ion.

Conclusions

We have shown that the family of heterotrinuclear complexes $[\text{Ni}(\text{H}_2\text{L})_2][\text{CoCu}(\text{L})_2(\text{H}_2\text{L})(\text{NCS})]_2(\text{NCS})_2$ **1**, $[\text{Ni}(\text{H}_2\text{L})_2][\text{CuCo}(\text{L})_2(\text{H}_2\text{L})(\text{NCS})]_2\text{Br}_2 \cdot 2\text{H}_2\text{O}$ **2**, and $[\text{CuCoCd}(\text{H}_2\text{L})_2(\text{L})_2(\text{NCS})\text{Br}_2] \cdot \text{CH}_3\text{OH}$ **3** can be readily prepared in nonaqueous solvent through the reaction of zerovalent copper, two different metal salts (Co and Ni or Co and Cd), and diethanolamine in open air. These complexes demonstrate that metal aminoalkoxo species generated in solution can be used to assemble discrete molecular architectures featuring three different transition metal atoms in which the ligand acts to bridge metal centers utilizing either coordinate interactions or complementary hydrogen bonds. The purpose of this work at the outset was to establish the factors that might lead to the formation of heterotrinuclear complexes and influence their overall aggregate architecture. An explanation for the elaborate molecular organization found should rest on a combination of the covalent-bond-forming capabilities of the metal ions involved and the molecular topologies of the metal aminoalkoxo modules bearing a set of hydrogen-bond donor/acceptor sites. Although the com-

(13) (a) Koerner, R.; Ölmstead, M. M.; Ożarowski, A.; Phillips, S. L.; Van Calcar, P. M.; Winkler, K.; Balch, A. L. *J. Am. Chem. Soc.* **1998**, *120*, 1274–1284. (b) Baranowski, J.; Cukierda, T.; Jeżowska-Trzebiatowska, B.; Kozłowski, H. *Chem. Phys. Lett.* **1976**, *39*, 606. (c) Ożarowski, A.; Reinen, D. *Inorg. Chem.* **1986**, *25*, 1704.

pounds undergo fragmentation in solution, the fact that the components of **1** and **2** readily self-assemble to form crystals and can be easily recrystallized from polar MeOH suggests considerable stability for the selective triple-hydrogen-bonded interaction arising from the particular arrangement of H-bond donor (D) and acceptor (A) sites



that ensure the thermodynamic stability of the heterotri-metallic lattice.

Acknowledgment. This work was supported in part by the INTAS (Project 03-51-4532). We are grateful to Professor J. Sieler for X-ray data collection for one of the compounds.

Supporting Information Available: Crystallographic data in CIF format. This material is available free of charge via the Internet at <http://pubs.acs.org>.

IC048955W